J. Phys. IV France **11** (2001)

Nanoscale cobalt oxides thin films obtained by CVD and sol-gel routes

L. Armelao, D. Barreca[1], S. Gross[1] and E. Tondello[1]

CNR-CSSRCC, Department of Inorganic, Metallorganic and Analytical Chemistry, University of Padova, Via Marzolo 1, 35131 Padova, Italy
[1] *Department of Inorganic, Metallorganic and Analytical Chemistry, University of Padova, Via Loredan 4, 35131 Padova, Italy*

Abstract. *The effect of the preparation procedure on the structure and properties of nanoscale systems constitutes an interesting starting point for the preparation of advanced materials for functional applications. In this work, cobalt oxides nanocrystalline thin films were synthesized by the Chemical Vapor Deposition and sol-gel routes. In the first case, a Co(II) β-diketonate was employed as source compound in an oxygen atmosphere, whereas the sol-gel films were obtained by dip-coating from alcoholic solutions of cobalt acetate. The films were deposited on glassy substrates (SiO_2, Indium Tin Oxide) and subsequently annealed in different conditions in order to tailor their composition from CoO to Co_3O_4 by a proper combination of the synthesis parameters and thermal treatments. The microstructure of the samples was studied by X-ray Diffraction (XRD) and optical absorption, while their surface and in-depth chemical composition was analyzed by X-ray Photoelectron (XPS) and (XE-AES) techniques. Atomic Force Microscopy (AFM) was employed to analyze the surface morphology of the films. Particular emphasis was given to the influence of the preparation route on the system features by a comparison of the results obtained by the two synthetic approaches.*

1. INTRODUCTION

Thin films of the principal cobalt oxides, NaCl-type CoO and spinel-type Co_3O_4, have been the subject of thorough investigations for different applications, such as solar thermal absorbers, protective layers and magneto-optical recording media [1]. Besides, they have been used in the preparation of heterogeneous catalysts [2], as electrodes for catalytic processes [3] and as high-capacity energy storage systems [4]. In recent years, much attention has been paid to Co-O based films for the production of optical gas sensing [5,6] and electrochromic devices, where they have been used either as active elements (Co_3O_4) [7] or as counter-electrodes (CoO) [8].

The interest towards these systems has been strongly increased by the outstanding importance displayed by nanoscale films and clusters, that show unique chemical and physical properties thanks to their high surface-to-volume ratio. For instance, size effects play an important role in the fields of catalysis, gas sensors and magnetism, where the material properties are strongly influenced by the surface defects, grain size distribution and particle mutual interactions [9]. On these basis, great research efforts have been devoted to the development of proper synthetic routes for the preparation of systems with tailored properties. In the widespread scenario of thin film deposition techniques, Chemical Vapor Deposition and Sol-gel processes are suitable for the preparation of nanoscale thin films due to operative soft conditions, where the first nucleation stages are favored over the subsequent material growth [10]. Further interesting perspectives rely on the chemical control of the system properties, which can be attained by a proper combination of the molecular precursor and the synthesis parameters.

Following a previous work on RuO_2-based nanosystems [11], the aim of this paper is to highlight the importance of a comparative approach in the CVD and sol-gel preparation of Co-O based coatings, examining the influence of the synthesis and treatment conditions on their composition, microstructure and morphology.

We have recently reported the CVD synthesis and characterization of cobalt oxide based coatings with controlled composition using a Co(II) β-diketonate, $Co(dpm)_2$ (Hdpm = 2,2-6,6-tetramethyl-3,5-heptanedione) as a novel precursor [12]. Besides the appreciable volatility, the advantages offered by this compound are the absence of direct Co-C bonds, that reduces the possibility of carbon contamination, and the presence of thermally labile Co-O moieties, that can be attacked in oxidizing atmosphere with formation of volatile byproducts.

The preparation of the sol-gel films has been accomplished starting from methanolic solution of $Co(OCOCH_3)_2{\cdot}4H_2O$ and subsequent treatments in oxidizing or reducing atmospheres at different temperatures [13]. In this case, the precursor choice was linked to the clean thermal decomposition of cobalt acetate, which does not leave residual contaminants inside the coatings.

The films were deposited on Indium-Tin Oxide (ITO), a transparent conductor, and on silica slides, in view of future applications of the layers as active elements in electrochromic devices and/or optical sensors. Since both substrates are basically glasses, negligible influence on morphological and textural features were expected. The microstructure (XRD, optical absorption), surface and in-depth composition (XPS and XE-AES) and surface morphology (AFM) were characterized in detail. The aim of this paper is to summarize the most relevant analogies and differences of the systems obtained by CVD and sol-gel routes, with particular attention to the influence of the precursor and the process parameters on the chemico-physical properties of the obtained films. The attention will be also focused on the selective synthesis of CoO, Co_3O_4 or mixed phase nanosystems by suitable variations of the process conditions.

2. EXPERIMENTAL

2.1 Film preparation

The CVD films were deposited on ITO by means of a cold-wall low-pressure CVD reactor with a resistively heated susceptor. Electronic grade O_2 was used as carrier and reactive gas. The precursor $Co(dpm)_2$ (whose synthesis and characterization were already reported [12]) was placed in a vaporization vessel connected to the reactor tube and maintained at 90°C throughout each film deposition. The gas-line and valves between the vessel and the reaction tube were heated to avoid condensation of the precursor. The pressure was measured by a capacitance manometer and the gas flow was controlled by a mass-flow controller (MKS instruments). In order to investigate the influence of process parameters on the film characteristics, two sample sets were obtained by CVD: **(I)** $p(O_2)$=10 mbar, O_2 flow rate=150 sccm; **(II)** $p(O_2)$=2 mbar, O_2 flow rate=50 sccm. In both cases the growth temperature was varied between 350 and 500°C.

The sol-gel films were deposited on silica slides starting from solutions of $Co(OCOCH_3)_2{\cdot}4H_2O$ in methanol with a molar ratio Co/CH_3OH= 1:35 [13]. The mixture was stirred for 10 minutes at room temperature and subsequently used for film deposition by dip coating (withdrawal speed = 5 $cmxmin^{-1}$). The samples were then annealed *ex-situ* in air, in nitrogen and in H_2/Ar (33% H_2) stream for one hour at temperatures ranging between 300 and 900° C, in order to investigate both structural and compositional evolution as a function of annealing atmosphere and temperature.

Before film preparation, the ITO (indium tin oxide, In_2O_3:Sn, ρ=10 Ω/square) [12,14] and Herasil silica (Heraeus) substrates were cleaned by a particular procedure [15] and dried in air. Prior to the deposition of the CVD films, the substrates were heated in the reactor chamber by flowing O_2 for 40' at the deposition temperature. Estimation of coating thickness was performed by an Alpha-Step 200 Tencor profilometer. For the CVD films, the obtained values range from 200 nm (CoO coatings) to

1200 nm (Co_3O_4 films grown at 500°C, set **(II)**, $p(O_2)$=2 mbar, O_2 flow rate=50 sccm). The thickness of the sol-gel films ranged between 20 and 50 nm.

2.2 Film characterization

XRD patterns were recorded using a Philips PW 1820 diffractometer (CuKα radiation, 40 kV, 50 mA) equipped with a thin film attachment (glancing angle=0.5°). The average crystallite dimensions were estimated by means of the Scherrer equation.

XPS and XE-AES analyses were carried out in a Perkin Elmer Φ 5600ci spectrometer, using a monochromatized AlKα radiation (1486.6 eV) for the CVD films and a standard MgKα source (1253.6 eV) for the sol-gel films. The working pressure was less than $1.8x10^{-9}$ mbar. The spectrometer was calibrated by assuming the binding energy (BE) of the Au $4f_{7/2}$ line at 84.0 eV with respect to the Fermi level. Charging effects were corrected assigning to the C1s signal of adventitious carbon the BE value of 285.0 eV [16]. The estimated standard deviation is ±0.2 eV. Detailed scans were recorded for the following regions: O1s, C1s, Co2p, CoLMM. After a Shirley-type background subtraction, the raw spectra were fitted using a non-linear least-square fitting program adopting Gaussian-Lorentzian shapes for all the peaks. The atomic compositions were evaluated using sensitivity factors as provided by Φ V5.4A software. Depth profiles were carried out by Ar^+ sputtering at 3.0 kV, 0.4 $\mu Axcm^{-2}$ beam current density with an argon partial pressure of $4x10^{-8}$ mbar.

The optical absorption spectra of the films were recorded on a Cary 5E (Varian) UV-Vis-NIR dual-beam spectrophotometer, operating in transmittance mode at normal incidence.

AFM images were taken using a Park Autoprobe CP instrument operating in contact mode in air. The background was subtracted from the images using the ProScan 1.3 software from Park Scientific.

3. RESULTS AND DISCUSSION

Cobalt oxide films obtained either *via* CVD or *via* sol-gel resulted homogeneous, crack-free and well adherent to the substrates. While Co_3O_4-containing coatings were all bluish-brown, CoO layers appeared yellow-gray.

For both sample sets, the microstructure appears to be little influenced by prolonged exposure to the outer atmosphere. All the CVD films belonging to set **(I)** ($p(O_2)$=10 mbar, O_2 flow rate=150 sccm) showed the typical XRD reflections of cubic Co_3O_4 [17], with no appreciable preferential orientation (see fig. 1, line **B**). Similar diffraction patterns were obtained for the samples belonging to set **(II)** ($p(O_2)$=2 mbar, O_2 flow rate=50 sccm) deposited at temperatures higher than 450°C. Conversely, the film deposited at 350°C belonging to set **(II)** was formed of pure CoO [18] (see fig. 1, line **A**). In this spectrum the ITO reflections (marked with *) are probably observed due to the low crystallinity of the monoxide layer. Finally, the film of set **(II)** deposited at 400°C showed reflections due to CoO and Co_3O_4, thus suggesting the presence of both oxides.

The as-deposited sol-gel coatings obtained by dipping from the methanolic solution of the Co(II) salt were firstly treated in air and nitrogen at different temperatures. In both cases the formation of crystalline CoO was not achieved, whatever the firing temperature. The diffraction pattern for the samples treated in N_2 (Fig. 1, line **D**) showed the presence of crystalline Co_3O_4 [17] already after heating at 300° C. On the basis of these results, the synthesis of CoO films was attempted by annealing the as-grown samples in reducing atmosphere (H_2/Ar). In this case, treatments between 300 and 500° C resulted in the formation of crystalline CoO [18] (Fig. 1, line **C**), while higher treatment temperatures induced the formation of metallic cobalt [13]. Annealing at 700° C caused the complete reduction of Co(II) to nanocrystalline Co(0) (grain size ≈20 nm).

The average crystallite size, computed from the width of the most intense peaks of each spectrum, indicates that both CVD and sol-gel routes gave rise to nanoscale films, with a fine control on the

coating microstructure depending on the synthetic route. The average cluster size ranged from 13-28 nm for CVD films, with the lowest values (13 nm) for CoO samples. This observation was explained by hypothesizing that CoO formation from the vapor phase on ITO was slower than that of Co_3O_4, limiting the grain growth after the first nucleation stages [12]. In the case of Co_3O_4 films prepared *via* sol-gel, the crystallite dimensions ranged from 7 to 15 nm on going from the 300 to the 500° C treated coatings, indicating that higher temperatures promoted the growth of oxide grains. For the CoO film treated at 500°C in H_2/Ar, the average value (≈11 nm) resulted similar to that of the CVD films with the same composition. In summary, the system microstructure results affected by the processing conditions.

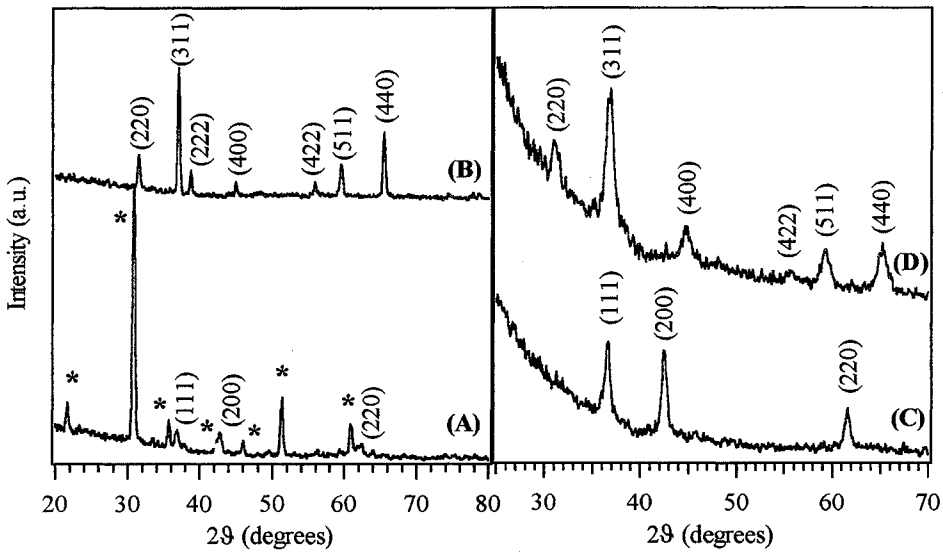

Figure 1. XRD diffraction patterns for some selected CVD (**A**, **B**) and sol-gel (**C**, **D**) samples: (**A**) CoO (set **(II)**; T= 350°C, $p(O_2)$=2 mbar, O_2 flow rate=50 sccm); (**B**) Co_3O_4 (set **(I)**; T= 500°C, $p(O_2)$=10 mbar, O_2 flow rate=150 sccm); (**C**) CoO (annealed at 500°C in H_2/Ar, 1h); (**D**) Co_3O_4 (annealed at 300°C in N_2, 1h). The reflections for the detected oxides are indexed in the corresponding patterns. Peaks marked with * are due to the ITO substrate.

The composition of the films and the in-depth distribution of the species were investigated combining XPS and XE-AES techniques. As a matter of fact, the binding energy (BE) values of the most intense Co signal (Co2p) are very similar for CoO [pure Co(II)] and Co_3O_4 [$Co(II)Co(III)_2O_4$] [19]. Nevertheless, the former is characterized by an intense satellite shake-up structure and its presence can be further confirmed by the evaluation of the Auger parameter[i] [20].

In the case of CVD samples, except for the one deposited at 350°C belonging to set **(II)**, the surface $Co2p_{3/2}$ BE (≈780.0 eV, Full Width at Half Maximum (FWHM) = 3.3 eV) and the Auger parameters (≈1553.2 eV) were in agreement with those reported for Co_3O_4 (Fig. 2a) [21]. Similar features were detected for the sol-gel samples annealed in both air and nitrogen. Conversely, in the CVD film obtained at 350°C belonging to set **(II)** (T=350°C; p=2 mbar) the $Co2p_{3/2}$ BE (≈780.4 eV, FWHM = 4.2 eV) was slightly higher and the signal was characterized by intense shake-up peaks at ≃ 5.4 eV from the spin-orbit components. This satellite structure was used as a fingerprint for the recognition of Co(II) species in CoO [22]. The presence of this oxide was confirmed by the $Co2p_{3/2}$-$Co2p_{1/2}$ energy splitting (16.0 eV) and the Auger parameter (1554.2 eV) [23], indicating that pure cobalt monoxide could be obtained only in mild oxidative conditions. Concerning the sol-gel films, the

[i] The Auger parameter was calculated by the sum of the $Co2p_{3/2}$ binding energy (BE) and the CoLMM Auger peak kinetic energy (KE).

presence of pure CoO (Fig. 2b) was evidenced by XPS spectra for samples annealed in H_2/Ar up to 500°C, in agreement with XRD data.

The results of XPS and XE-AES confirmed those obtained by XRD, except for the CVD coating of set **(II)** grown at 400°C whose diffraction pattern displayed the presence of both the oxides. This phenomenon could be explained supposing that CoO was formed in the first nucleation stages and subsequently oxidized to the more stable Co_3O_4 in the outer grain layers [12].

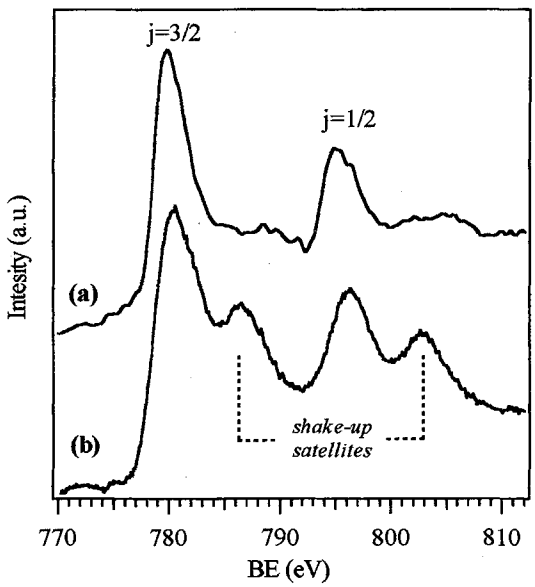

Figure 2. Co2p photoelectronic surface signals for : **(a)** a Co_3O_4 film obtained *via* CVD on ITO substrate (set **(I)**; T= 500°C, $p(O_2)$=10 mbar, O_2 flow rate=150 sccm); **(b)** a CoO film synthesized *via* sol-gel on silica glass (annealed at 500°C in H_2/Ar, 1h).

For both CVD and sol-gel samples, the O1s surface peak displayed a significant broadening towards high BEs and was resolved in three different components. The first, at $\simeq$ 529.6 eV, was typical for cobalt oxide networks; the second ($\simeq$ 531.5 eV) was related to the presence either of hydroxyl species or of coordinative unsaturated oxygen, and the third ($\simeq$ 533.0 eV) to adsorbed water [12,16]. The disappearance of the last two bands after a mild sputtering in the case of the CVD films indicated that they arose from exposure to the outer atmosphere. Concerning the sol-gel films, the contribution of the 531.5 eV component is detected even in the inner layers, especially for films annealed at T<500°C, indicating that their solid network probably contains –OH groups in the Co coordination polyhedra.

The in-depth distribution of the species was analyzed by XPS depth profiles. Irrespective of the preparation route, the atomic Co and O percentages were almost constant from the surface to the substrate interface, indicating an homogeneous composition. As a matter of fact, for both CVD and sol-gel samples a near-substrate region containing both films and support signals was observed and related either to the interface roughness or to the grain nanostructure. The main difference between CVD and sol-gel films was due to the presence of hydrocarbon residuals. Whereas for all the CVD films the carbon contamination was limited to the outermost layers, in the case of sol-gel Co_3O_4 samples fired at 300°C contaminants were evidenced also inside the films and the complete decomposition of the Co(II) precursor occurred at annealing temperatures greater than 400°C.

Since the ligand field absorption may be very sensitive to the local Co-O coordination, the optical absorption properties were used as a probe for the effect on this coordination of synthesis parameters.

Indeed, the obtained results revealed that spectral features were mainly influenced by film composition rather than on the synthesis procedure. In the case of Co_3O_4 layers, four different bands were always identified (fig. 3a) and assigned as follows:

i) A band ($\lambda \approx 1520$ nm) $\Rightarrow$ crystal field $^4A_2(F) \rightarrow {}^4T_1(F)$ transitions in the Co_3O_4 structure [24];

ii) B band ($\lambda \approx 1270$ nm) $\Rightarrow$ Metal-Metal Charge Transfer Co(II)$\leftrightarrow$Co(III) [25];

iii) C ($\lambda \approx 730$ nm) and D ($\lambda \approx 440$ nm) bands $\Rightarrow$ Ligand-Metal Charge Transfer (LMCT) events (O(-II)$\rightarrow$Co(III) and O(-II)$\rightarrow$Co(II) respectively).

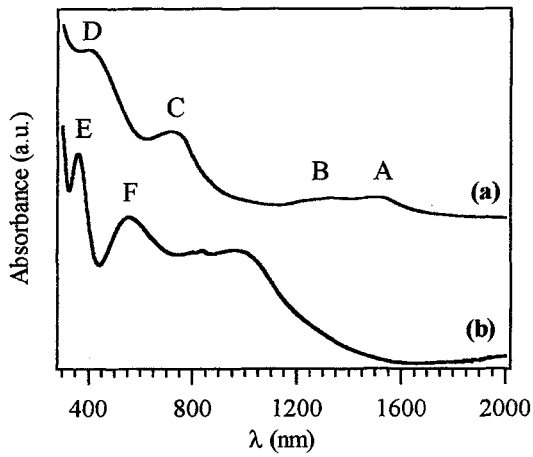

Figure 3. Optical absorption spectra for: **(a)** a Co_3O_4 film obtained *via* sol-gel on silica glass (annealed at 300°C in air, 1h); **(b)** a CoO film synthesized *via* CVD on ITO substrate (set **(II)**; T= 350°C, $p(O_2)$=2 mbar, O_2 flow rate=50 sccm).

A different spectral profile was detected for the CoO films prepared by both CVD and sol-gel routes (see fig. 2b for the CVD sample). In particular, the band at 357 nm (E) was attributed to LMCT processes O(-II)$\rightarrow$Co(II), and the absorption centered at 550 nm (F) was ascribed to Co(II) transitions in octahedral crystal field [26]. In agreement with the previous analyses, the CVD coating of set **(II)** grown at 400°C (spectrum not reported) confirmed the presence of both CoO and Co_3O_4 also in the optical spectrum.

The surface morphology of the layers and its dependence on the synthesis conditions was analyzed by AFM. In the case of CVD films, no appreciable differences were detected on going from CoO to Co_3O_4 films (fig. 4a). In fact, the film surface was always characterized by the presence of globular grains (ϕ=340÷580 nm). For each deposition set, the increase of the substrate temperature corresponded to the increase of the grain size and the average roughness (from $\approx$5 to $\approx$30 nm). Concerning the sol-gel samples, a more pronounced difference was detected between CoO and Co_3O_4 films. Even if the grain size was very similar (ϕ=150÷200 nm), in the case of sol-gel Co_3O_4 samples the agglomerates are grouped together to form cross-linked lengthened-shaped structures. For the CoO films (see fig. 4b), an average roughness of 11 nm is estimated. In all cases, the grains observed in the AFM micrographs can be considered as nanocrystallite aggregations (compare with grain dimensions estimated from the XRD analysis).

4. CONCLUSIONS

A comparative approach to the synthesis of cobalt oxide thin films has been proposed by CVD and sol-gel routes. In the first case, $Co(dpm)_2$ was chosen as precursor, whereas sol-gel coatings were

obtained starting from $Co(OCOCH_3)_2 \cdot 4H_2O$. The obtained results show that both approaches were successful in obtaining nanocrystalline films with a composition ranging from CoO to Co_3O_4, which is the most stable form in ordinary conditions. In the case of CVD synthesis, a main advantage of the used precursor was the possibility of tailoring its decomposition by varying the oxygen content in the reaction atmosphere. CoO was obtained by CVD only at 350°C and total pressure $p(O_2)$=2 mbar. Conversely, its formation *via* sol-gel required an *ex-situ* thermal curing in H_2/Ar atmosphere up to 500°C. Heating at higher temperatures in the same atmosphere induced the reduction of Co(II) to metallic cobalt, while annealing in air and N_2 induced the formation of Co_3O_4 coatings. A possible explanation to this last result is that also a very low oxygen amount, the one present in N_2, is sufficient to oxidize Co(II) to Co(III), giving thus Co_3O_4. Surface and in-depth XPS analyses indicated that a careful control of the synthesis conditions allowed to obtain a clean conversion of the used precursors to cobalt oxides with a good compositional homogeneity. While the optical spectra of the films were influenced mainly by their composition, the surface morphology appeared dependent on the preparation procedure, which affects the nucleation events during film growth.

Interesting perspectives for the development of this work would concern the influence of the preparation route on the functional properties of the layers in electrochromic devices and gas sensors.

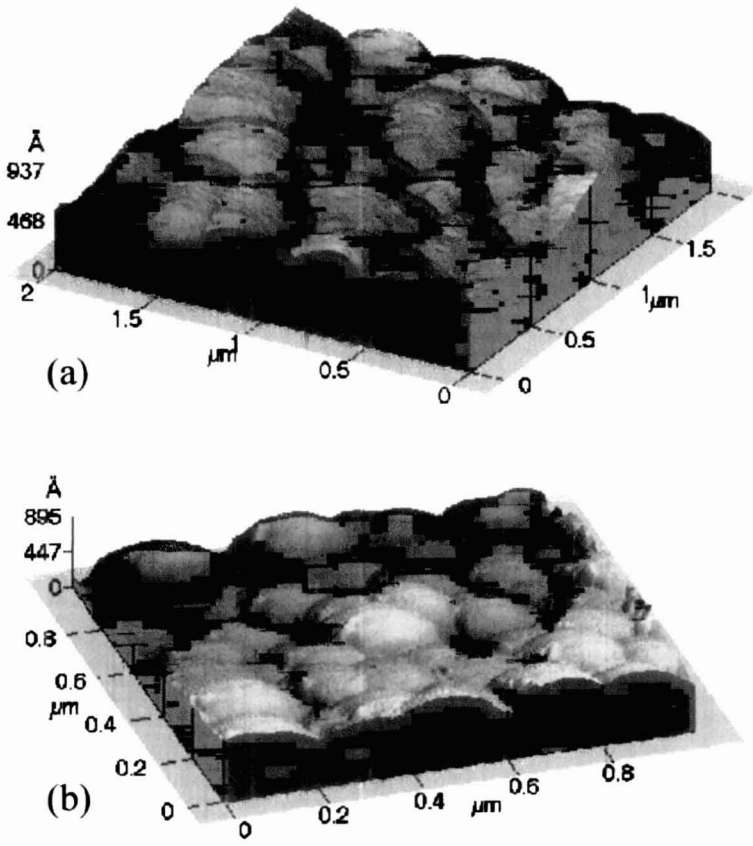

Figure 4. AFM 3D surface micrographs for: **(a)** a Co_3O_4 film (2μmx2μm) synthesized *via* CVD on ITO substrate (set **(I)**; $p(O_2)$=10 mbar, O_2 flow rate=50 sccm); **(b)** a CoO film obtained *via* sol-gel on silica glass (annealed at 500°C in H_2/Ar, 1h).

Special thanks are due to dr. A. Martucci and prof. P. Colombo (Dipartimento di Ingegneria Meccanica-Sez. Materiali-Università di Padova) for the XRD measurements.

References

[1] See for instance: (a) Cook J.G., Koffyberg F.P., *Sol. Energy Mater.* **10** (1984) 55; (b) Barrera E., Gonzales I. and Viveros T., *Solar Energy Mater. and Solar Cells* **51** (1998) 69; (c) Nasu S., Matsumoto K., Hashimoto K. and Saiki K., *IEEE Trans. Magn.* **MAG-23** (1987) 2257.

[2] (a) Hamada H., Haneda M., Kakuta N., Miura H., Inomi K., Nanba T., Qi Hua W., Veno A., Ohfune H. and Udagawa Y., *Chem. Letters* (1997) 887; (b) Weichel S., Møller P.J., *Surf. Sci.* **399** (1998) 219; (c) Koyano G., Watanabe H., Okuhara T. and Misono M. *J. Chem. Soc. Faraday Trans.* **92** (1996) 3425.

[3] Nkeng P., Koening J., Gautier J., Chartier P. and Poillerat G., *J.Electroanal. Chem.* **402** (1996) 81.

[4] Ramachandran K., Oriakhi O., Lerner M.M. and Koch V.R. *Mater. Res. Bull.* **31** (1996) 67.

[5] Ando M., Kobayashi T., Iijima S. and Harita M., *J. Mater. Chem.* **7** (1997) 1779.

[6] Yamaura H., Tamaki J., Moriya K., Miura N. and Yamazoe N., *J. Electrochem. Soc.* **144** (1997) L158.

[7] Maruyama T., Arai S., *J. Electrochem. Soc.* **143** (1996) 1383.

[8] Monk P.M.S., Chester S.L., Higham D.S. and Partridge R.D., *Electrochim. Acta* **39** (1994) 2277.

[9] Soriano L., Abbate M., Fernández A., González-Elipe A.R., Sirotti F., and Sanz J.M., *J. Phys. Chem. B* **103** (1999) 6676.

[10] (a) Spencer J.T., *Progr. Inorg. Chem.* **41** (1994) 145; (b) Brinker C.J., Scherer G.W., in: *Sol-Gel Science: The Physics and Chemistry of Sol-Gel Processing* (Academic Press, New York, 1990).

[11] Armelao L., Barreca D. and Moraru B., *Thin Solid Films*, submitted.

[12] Barreca D., Massignan C., Daolio S., Fabrizio M., Piccirillo C., Armelao L. and Tondello E., *Chem. Mater.*, **13** (2001) 588.

[13] Armelao L., Barreca D., Gross S., Martucci A., Tieto M. and Tondello E., *J. Non-Cryst. Solids*, accepted for publication.

[14] Svegl F., Orel B., Hutchins M.G. and Kalcher K., *J. Electrochem. Soc.* **143** (1996) 1532.

[15] Armelao L., Bertoncello R., Coronaro S. and Glisenti A., *Science and Technology for Cultural Heritage* **7** (1998) 41.

[16] Moulder J.F., Stickle W.F., Sobol P.W. and Bonben K.D., *Handbook of X-ray Photoelectron Spectroscopy* (Perkin-Elmer, Eden Prairie, MN, 1992).

[17] Patterns No. 42-1467 and 43-1003, *JCPDS-ICDD*, 1992.

[18] Pattern No. 43-1004, *JCPDS-ICDD*, 1992.

[19] Strydom C.A., Strydom H.J., *Inorg. Chim. Acta* **159** (1989) 191.

[20] Haber J., Ungier L., *J. Electron Spectrosc. Relat. Phenom.* **12** (1977) 305.

[21] For instance: (a) Oku M., Hirokawa K., *J. Electron Spectrosc. Relat. Phenom.* **8** (1976) 475; (b) Ramsey M.G., Russell G.J., *Appl. Surf. Sci.* **22/23** (1985) 206.

[22] McIntyre N.S., Johnston D.D., Coatsworth L.L., Davidson R.D. and Brown J.R., *Surf. Interf. Anal.* **15** (1990) 265.

[23] Khawaja E.E., Durrani S.M.A., Al-Adel F.F., Salim M.A. and Sakhawat Hussain M., *J. Mater. Sci.* **30** (1995) 225.

[24] Nkeng P., Poillerat G., Koenig J.F.; Chartier P., Lefez B., Lopitaux J. and Lenglet M., *J. Electrochem. Soc.* **142** (1995) 1777.

[25] Ruzakowski Athey P., Urban III F.K., Tabet M.F. and McGahan W.A., *J. Vac. Sci. Technol. A* **14** (1996) 685.

[26] Duran A., Fernandez Navarro J.M., Casariego P. and Joglar, A., *J. Non-Cryst. Solids* **82** (1986) 391.